Differential sintering of Al$_2$O$_3$/ZrO$_2$–Ni composite, during pulse electric current sintering

Dongming Zhang [a,*], Lianmeng Zhang [a], Zhengyi Fu [a], Jingkun Guo [a], Wei-Hsing Tuan [b]

[a] *State Key Laboratory of Advanced Technology for Materials Synthesis and Processing, Wuhan University of Technology, Wuhan 430070, China*
[b] *Department of Materials Science and Engineering, National Taiwan University, Taipei 106, Taiwan*

Abstract

Powder mixtures of Al$_2$O$_3$, ZrO$_2$, Ni were sintered by pulse electric current sintering at 1300 °C with a heating rate of 200 °C/min or 130 °C/min. Large ZrO$_2$–Ni agglomerates are formed within the Al$_2$O$_3$ matrix after sintering. Depending on the heating rate, these agglomerates formed networks within the matrix. The networks are heterogeneously distributed in the specimens prepared by the heating rate of 200 °C/min but homogeneously in the specimens prepared by the heating rate of 130 °C/min. The microstructure evolution of the specimen prepared by the heating rate of 200 °C/min indicates that the temperature at the edge of the specimen is higher than that at the center. The temperature difference is smaller for the specimen prepared by the heating rate of 130 °C/min. The small ZrO$_2$ particles tend to associate with nickel melt to form ZrO$_2$–Ni agglomerates. Then the ZrO$_2$–Ni agglomerates are migrated by magnetic field that induced by the pulse electric current.

© 2005 Elsevier Ltd and Techna Group S.r.l. All rights reserved.

Keywords: Pulse electric current sintering; Microstructure; Al$_2$O$_3$–ZrO$_2$–Ni; Differential sintering

1. Introduction

The applications of ceramics as structural components are restricted because of their poor mechanical performance. To improve the mechanical properties of ceramics has thus attracted much attention. One of the most promising approaches is incorporating second-phase reinforcement into ceramic matrix [1]. The second-phase reinforcement can be either a ceramic or a metallic phase. The presence of the second-phase inclusions can prohibit the propagation of cracks and thus enhance the toughness of ceramics. By reducing the size of the second-phase particles below 100 nm, the strength of ceramic can also be enhanced significantly [2]. Among the many second-phase reinforcements used in previous studies, zirconia particles and nickel particles have received wide attention [3–5]. It is mainly because zirconia and nickel particles are readily available.

Furthermore, the addition of either zirconia or nickel particles can enhance both the strength and toughness of ceramics [3–5]. Recent studies suggested that the toughness of the brittle material can be increased by adding zirconia and metallic particles simultaneously [6–8]. For example, the toughness of an Al$_2$O$_3$/(ZrO$_2$ + Ni) composite could reach a value as high as 10 MPa m$^{0.5}$ [6]. However, the strength of the composite is only marginally enhanced. The Ni inclusions in the composite are relatively large, varying from 2.3 μm to 4.9 μm. The size may be large enough to induce micro-crack at interface because of the presence of thermal expansion mismatch between Al$_2$O$_3$ and Ni. By reducing the size of Ni particles, the strength of Al$_2$O$_3$ may be enhanced significantly [5]. In the present study, both nanometer-sized Ni and submicrometer-sized ZrO$_2$ powders are added into an Al$_2$O$_3$ matrix.

Pulse electric current sintering (PECS) is a novel firing technique with the features of extremely fast heating rate and an external pressure [9]. On top of these features, a pulse electric current is applied simultaneously to the powder

* Corresponding author. Tel.: +86 27 87651839; fax: +86 27 87879468.
E-mail address: zhangdongming71@hotmail.com (D. Zhang).

compact. Many experimental evidences have demonstrated that the densification rate [9], grain growth rate [10] and creep rate [11] are enhanced by this technique. The technique has also demonstrated its merit in preparing nano-ceramics at a low sintering temperature with a short dwell time [12]. Yet its mechanism is not understood till now. Some investigators claimed that plasma or electrical discharge could be generated between particles during PECS [13]. Some suggested that the mechanism for pulse electric current sintering should be similar to that of hot-pressing [14,15]. Furthermore, there was no report on the transportation of particles during pulse electric current sintering, which will be demonstrated in the present study.

2. Experimental

2.1. Powder preparation

The detailed procedures for the preparation of the Al_2O_3/ZrO_2–Ni powder mixtures can be found in a previous study [16]. A brief description is given here. An alumina (TM-DAR, $d_{50} = 210$ nm, Taimei Chem. Co. Ltd., Tokyo, Japan) powder was mixed with 5 vol.% zirconia (TZ-3Y, $ZrO_2 + 3$ mol% Y_2O_3, $d_{50} = 230$ nm,

Tosoh Co., Japan) powder by ball milling in de-ionized water for 24 h. A separate solution of nickel nitrate $(Ni(NO_3)_2 \cdot 6H_2O$, Showa Chem. Co., Japan) was also prepared. The alumina and zirconia slurry was poured into the nickel nitrate solution and then stirred for 30 min. The resulting slurry was filtered, washed and dried. The powder mixtures were reduced in pure hydrogen at 550 °C for 1 h. The resulting Ni in the powder mixtures as determined by applying inductive coupled plasma mass spectrometry (ICP-MS) technique was 1 vol.% [16]. The size of the Ni particles was 10 nm.

2.2. Pulse electric current sintering (PECS)

The powders were densified in a graphite die with a PECS furnace (Dr. Sinter 1050 SPS, Sumitomo Coal Mining Co., Tokyo, Japan). The electrical pulse with 12:2 pulse sequence, 12 pulses with 3.3 ms for each pulse and followed by two periods of zero current, was used. An external pressure of 30 MPa was applied on the powder mixtures from the very beginning of the PECS process. The PECS was carried out at 1350 °C for 5 min with a heating rate of 130 °C/min and 1300 °C for 5 min with a heating rate of 200 °C/min. The final dimensions of the specimen were 20 mm in diameter and around 3–4 mm in thickness.
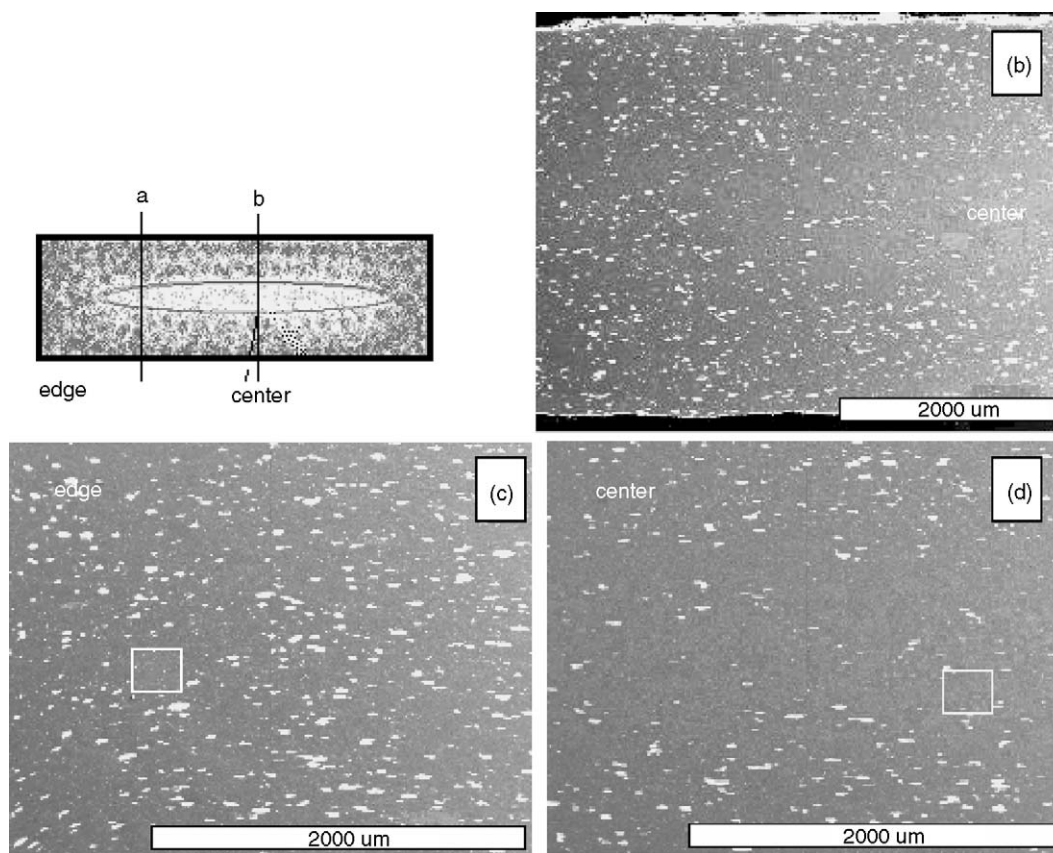

Fig. 1. The (a) schematic and (b–d) microstructure of the Al_2O_3/ZrO_2–Ni composite prepared by PECS at a heating rate of 200 °C/min. (b) The micrograph covers the area from the line a to the line b shown in (a). The micrographs in (c) is the edge area and in (d) central area.

2.3. Characterization

The cross section of the sintered samples were ground and polished with diamond pastes. The atomic distribution within the cross section was analyzed by using electron probe microanalysis (EPMA, JXA-8800R, Jeol Co., Tokyo, Japan).

3. Results

3.1. Specimen prepared with the heating rate of 200 °C/min

Fig. 1 shows the back-scattered electron images of the cross section of the Al_2O_3/ZrO_2–Ni composite prepared with the heating rate of 200 °C/min. Fig. 1(a) shows a schematic diagram to demonstrate the positions of the following micrographs. Fig. 1(b) shows a low-magnification micrograph which covers the center and part of edge area between line "a" and line "b" in Fig. 1(a). Large white agglomerates with the size about 80–100 μm can be found across the entire cross section. However, more large agglomerates are found in the edge area (Fig. 1(c)) than those in the central area (Fig. 1(d)). The shape of the agglomerate is ellipsoid in nature with its long axis perpendicular to the external load direction.

One of the large agglomerates is shown in Fig. 2. Apart from the agglomerate, white networks composing of small white particles are also found. The EMPA result of the large agglomerate is shown in Table 1. The EMPA results of the area shown in Fig. 1(c) and (d) are also shown in the table. The Ni content in Fig. 1(c) and (d) is very close to that in the starting powder mixtures. However, the Ni content in the agglomerates is two times that of the average Ni content.
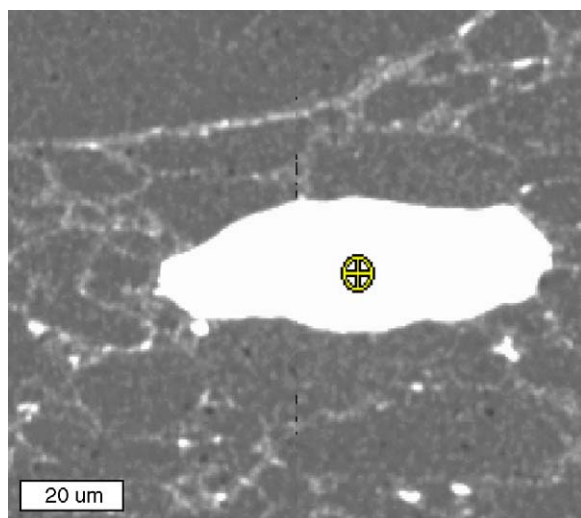

Fig. 2. A typical large ZrO_2–Ni agglomerate in the composite prepared by PECS at a heating rate of 200 °C/min. The dot indicates the position for the EMPA analysis. The EPMA result is shown in Table 1.

Table 1
The chemical composition of the Al_2O_3/ZrO_2–Ni composites as determined by EPMA

	Atomic percentage			
	O	Al	Ni	Zr
Fig. 1(c)	44.38	52.58	1.28	1.77
Fig. 1(d)	44.20	52.98	1.18	1.64
Fig. 2	44.85	0	2.23	52.93
Fig. 5(b)	44.17	52.99	1.20	1.64
Fig. 5(c)	44.03	53.00	1.27	1.70

Furthermore, there is no Al found within the agglomerate, indicating that the agglomerate is mainly composing of ZrO_2 and Ni.

Fig. 3 shows the back-scattered electron images (Fig. 3(a)) and secondary electron image (Fig. 3(b)) of the central area. This area corresponds to the square shown in Fig. 1(d). There is no large ZrO_2–Ni agglomerate in this area. The corresponding distribution of O, Al, Zr and Ni atoms are also shown in the figure. The Zr and Ni atoms are not overlapped with one another, though their positions are very close. The size of ZrO_2 particles in this area is about 5–8 μm, while the Ni particles 4–5 μm.

Fig. 4 shows the back-scattered electron image (Fig. 4(a)) and secondary electron image (Fig. 4(b)) of the edge area. This area corresponds to the square shown in Fig. 1(c). There is no large ZrO_2–Ni agglomerate in this area. The corresponding distribution of O, Al, Zr and Ni atoms is also shown in the figure. The white ZrO_2 particles with the size of 5–8 μm are found in the matrix but the size of Ni particles is less than 1 μm. The size of Ni particles changes from 5 μm in central to 1 μm in edge indicates that most of Ni particles melt in edge. The microstructure in central reflects the original powders state before sintering, but the microstructure in edge reflects the state after sintering. By comparing Fig. 3 with Fig. 4, it can be deduced that the temperature in edge area is higher than that in center area. The temperature difference is relatively high.

3.2. Specimen prepared with the heating rate of 130 °C/min

Table 1 shows the atomic percentage of O, Al, Ni and Zr in the specimen prepared with the heating rate of 130 °C/min. Fig. 5 shows the back-scattered electron image of the Al_2O_3/ZrO_2–Ni composite prepared with the heating rate of 130 °C/min. The micrograph shown in Fig. 5(a) covers the center area and part of the edge area. Large ZrO_2–Ni agglomerates distributed homogeneously within the matrix, as shown in Fig. 5(b) and (c). The micrographs with larger magnification corresponding the squares shown in Fig. 5(b) and (c) are shown in Fig. 5(d) and (e), respectively. Apart from the agglomerates, ZrO_2–Ni networks are also found in the center and edge areas. The average diameter of the networks is larger in the center area than that in the edge
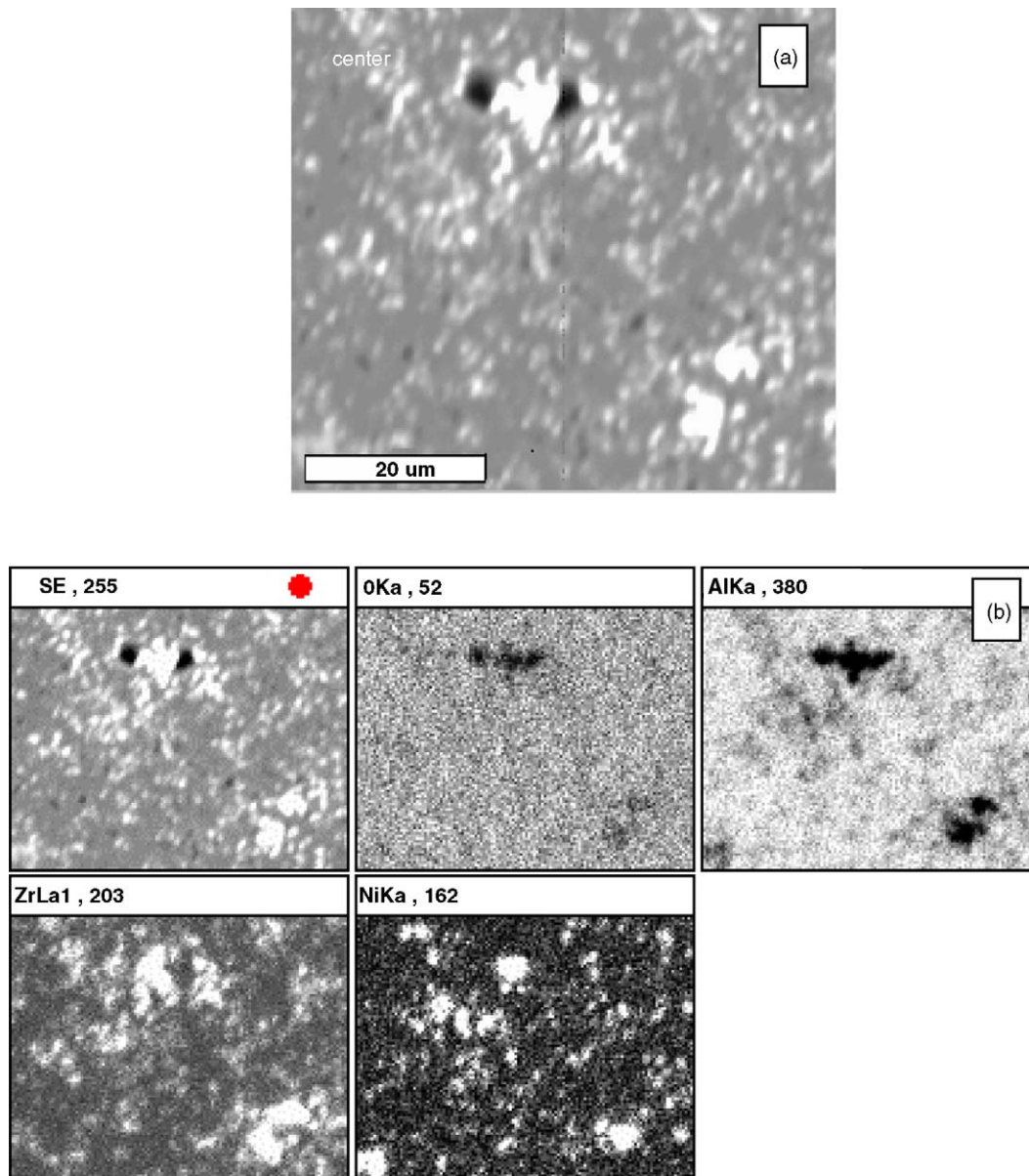
Fig. 3. The (a) back-scattered image and (b) secondary electron image of the central area in the composite prepared with a heating rate of 200 °C/min. The atomic mappings are also shown.

area. Besides, the amount of porosity in the center area is higher than that in the edge area. From the density variation, it indicates that the temperature is higher in edge area during pulse electric current sintering. Because large ZrO_2–Ni agglomerates distribute homogeneously and no 5 μm Ni particles are found in central area, indicating that the temperature difference from edge to center is not as high as that of the specimen prepared by the heating rate of 200 °C/min.

4. Discussion

By comparing the micrographs of the specimens prepared by the heating rate of 200 °C/min or 130 °C/min, some common and different points can be found. The common point lies on the fact that the temperature of the edge area is higher than that in the center temperature. The micro-structures of the specimens prepared by different heating rates are not the same, especially (1) the distribution of isolated and large ZrO_2–Ni agglomerates and (2) the distribution of small ZrO_2–Ni agglomerates and their networks. The large ZrO_2–Ni agglomerates are uniform in the specimens prepared with a lower heating rate but not uniform in the specimens prepared with a higher heating rate.

As far as the ZrO_2 networks is concerned, the diameter of ZrO_2 networks is about 30–60 μm. The grain size of Al_2O_3 in the central networks is around 1 μm as determined by SEM. So there are hundreds of Al_2O_3 grains within ZrO_2
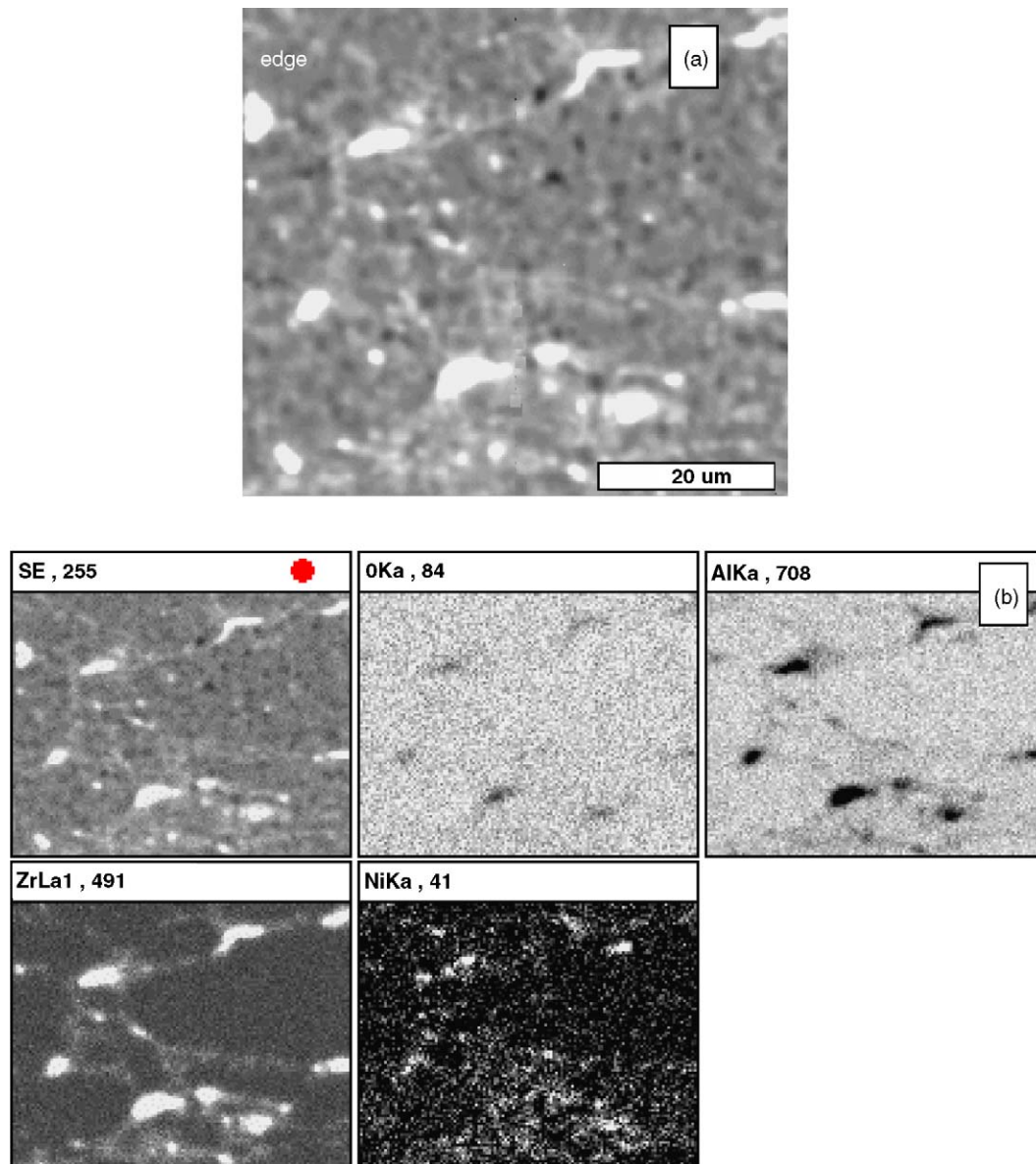
Fig. 4. The (a) back-scattered image and (b) secondary electron image of the edge area in the composite prepared with a heating rate of 200 °C/min. The atomic mappings are also shown.

networks. The size of ZrO_2 particles is 0.2 μm in the beginning. These small ZrO_2 particles are not located at the grain boundaries of Al_2O_3 matrix but form networks to surround many Al_2O_3 grains after sintering. It suggests that the ZrO_2 particles migrate a distance around 10–20 μm during pulse electric current sintering. The migration distance is far longer than the possible diffusion distance. It suggests that a mass transportation mechanism other than diffusion is active during PECS.

Due to the presence of ZrO_2 agglomerates and networks, it suggests that small ZrO_2 particles tend to ''attract'' each other. The random dispersion of ZrO_2 is transformed to partially ordered networks and agglomerates, an external force is needed. During PECS, a pulse electric current is applied onto the graphite mold. Such electric current can

induce a magnetic field. Table 1 demonstrates that the Ni content in the large ZrO_2 agglomerates is almost double that the Ni content in the matrix. The combination of ZrO_2–Ni particles may due to the melting of Ni. The melting point of Ni decreases as its size is in the nano-metered range [17,18]. Nickel may be melted during PECS since its starting size was only 10 nm. The wetting of Ni melt on Al_2O_3 and ZrO_2 is poor [19,20]. However, the wetting angle of Ni melt on ZrO_2 is slightly smaller than that of Ni melt on Al_2O_3. Therefore, Ni melt tends to combine with ZrO_2 during sintering.

Nickel is a ferromagnetic material. The presence of magnetic fields can offer the external force to move the ZrO_2–Ni particles. The existence of a magnetic field has never been proposed in previous studies on PECS. However,
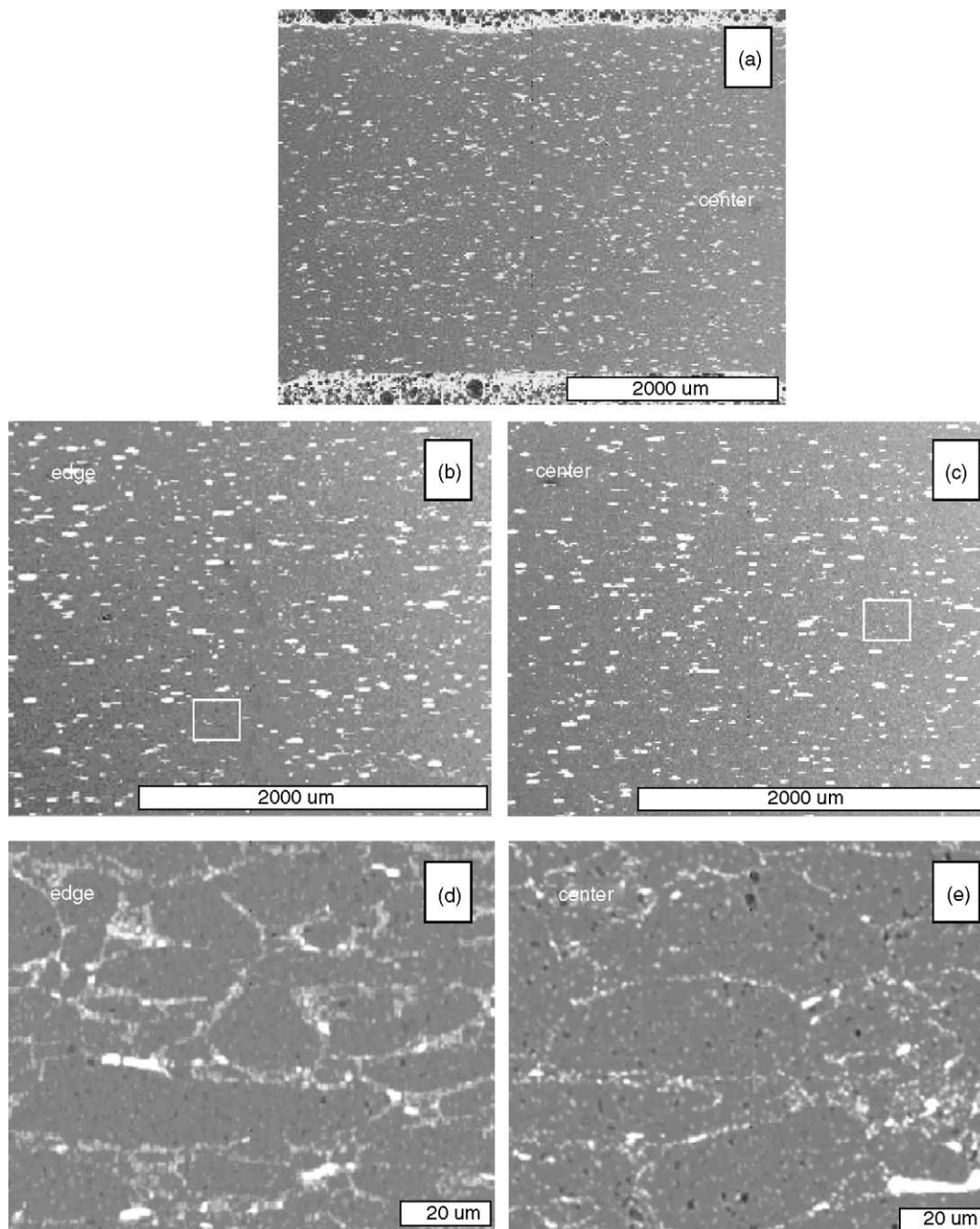
Fig. 5. The back-scattered images of the composite prepared with a heating rate of 130 °C/min. The micrograph (a) shows the microstructure at a low-magnification. The micrographs show the microstructure at the (b) edge and (c) central areas. The microstructures in the square in (b) and (c) are shown in (d) and (e), respectively.

a recent study suggested that the mechanism of PECS is similar to that of microwave sintering, which differs from previous study [21].

For the specimen prepared by the heating rate of 200 °C/min, the temperature in the center is relatively low. The Ni particles may not be melted; the small solid ZrO_2 and Ni particles are not associated to each other. They thus distribute uniformly in the central region. The temperature in the edge area is relatively high. The ZrO_2 and Ni particles are thus combined together due to Ni particles are melted.

The same reaction may also result in the formation of ZrO_2–Ni networks.

For the specimen prepared by the heating rate of 130 °C/min, the temperature in the central area is lower than that in the edge area, but the temperature variation is smaller than that in the specimen prepared by a faster heating rate. Most Ni particles in the central area are melted and associated with ZrO_2 particles. Larger ZrO_2–Ni agglomerates and networks are thus formed in the central and edge areas. Nevertheless, some Ni particles remain in

their solid state and are left behind in the matrix in the central area.

5. Conclusions

The following conclusions can be drawn from the present study.

(1) The temperature in the edge area is higher than that in the central area. The temperature difference is smaller as the heating rate is decreased.
(2) Large ZrO_2–Ni agglomerates and ZrO_2–Ni networks are formed due to the melting of nickel.
(3) The magnetic fields induced by the electric current can offer a force to migrate the ZrO_2–Ni small particles.
(4) For the specimens prepared by PECS with a heating rate of 200 °C/min, many large ZrO_2–Ni agglomerates are found mainly in the edge area. For the specimens prepared by the heating rate of 130 °C/min, large ZrO_2–Ni agglomerates are found in both edge and central areas.
(5) For the specimens prepared by PECS with a heating rate of 130 °C/min, large ZrO_2–Ni networks are found in the central area. For the specimens prepared by the heating rate of 200 °C/min, no ZrO_2–Ni networks are found in central area. Small ZrO_2 particles and Ni particles are dispersed uniformly in the matrix instead.

Acknowledgement

References

[1] A.G. Evans, Perspective on the development of high-toughness ceramics, J. Am. Ceram. Soc. 73 (1990) 187–206.
[2] K. Niihara, New design concept of structural ceramic–ceramic nanocomposite, J. Ceram. Soc. Jpn. 99 (1991) 974–982.
[3] R.H.J. Hannink, P.M. Kelly, B.C. Muddle, Transformation toughening in zirconia-containing ceramics, J. Am. Ceram. Soc. 83 (3) (2000) 461–487.
[4] W.H. Tuan, R.J. Brook, The toughening of alumina with nickel inclusions, J. Eur. Ceram. Soc. 6 (1990) 31–37.
[5] T. Sekino, T. Nakajima, S. Ueda, K. Niihara, Reduction, Sintering of a nickel-dispersed-alumina composite and its properties, J. Am. Ceram. Soc. 80 (5) (1997) 1139–1148.
[6] R.Z. Chen, Y.T. Chiu, W.H. Tuan, Toughening alumina with nickel and zirconia, J. Eur. Ceram. Soc. 20 (2000) 1901–1906.
[7] O. Sbaizero, S. Roitti, G. Pezzotti, R-curve behavior of alumina toughened with molybdenum and zirconia particles, Mater. Sci. Eng. A359 (2003) 297–302.
[8] M. Li, W.O. Soboyejo, Synergistic toughening of a hybrid NiAl composite reinforced with partially stabilized zirconia and molybdenum particles, Mater. Sci. Eng. A271 (1999) 491.
[9] S.W. Wang, L.D. Chen, T. Hirai, Densification of Al_2O_3 powder using spark plasma sintering, J. Mater. Res. 15 (2000) 982–987.
[10] Z. Shen, Z. Zhao, H. Peng, M. Nygren, Formation of tough interlocking microstructures in silicon nitride ceramics by dynamic ripening, Nature 417 (2002) 266–269.
[11] Z. Shen, H. Peng, M. Nygren, Formidable increase in the superplasticity of ceramics in the presence of an electric field, Adv. Mater. 15 (12) (2003) 1006–1009.
[12] M. Yoshimura, T. Ohji, M. Sando, Synthesis of nanograined ZrO_2-based composites by chemical processing and pulse electric current sintering, Mater. Lett. 38 (1999) 18–21.
[13] M. Tokita, Development of large-size ceramic/metal bulk FGM fabricated by spark plasma sintering, Mater. Sci. Forum 83 (1999) 308–311.
[14] S.W. Wang, L.D. Chen, T. Hirai, Effect of plasma activated sintering (PAS) parameters on densification of copper powder, Mater. Res. Bull. 35 (2000) 619–628.
[15] S.W. Wang, L.D. Chen, T. Hirai, Microstructure inhomogeneity in Al_2O_3 sintered bodies formed during the plasma-activated sintering process, J. Mater. Sci. Lett. 18 (1999) 1119–1121.
[16] W.H. Tuan, S.M. Liu, C.J. Ho, C.S. Lin, T.J. Yang, D.M. Zhang, Z.Y. Fu, J.K. Guo, Preparation of Al_2O_3–ZrO_2–Ni nanocomposite by pulse electric current and pressureless sintering, J. Eur. Ceram. Soc. 25 (2005) 3125–3133.
[17] A.N. Goldstein, C.M. Echer, A.P. Alivisatos, Melting in semiconductor nanocrystals, Science 256 (1992) 1425–1427.
[18] K.F. Peters, Y.W. Chung, J.B. Cohen, Surface melting on small particles, Appl. Phys. Lett. 71 (16) (1997) 2391–2393.
[19] P. Nikolopoulos, S. Agathopoulos, Interfacial phenomena in Al_2O_3-liquid metal and Al_2O_3-liquid alloy system, J. Eur. Ceram. Soc. 10 (1992) 415–424.
[20] D. Sotiropoulou, P. Nikolopoulos, Work of adhesion in ZrO_2-liquid metal systems, J. Mater. Sci. 28 (1993) 356–360.
[21] M. Suganuma, Y. Kitagawa, Pulsed electric current sintering of silicon nitride, J. Am. Ceram. Soc. 86 (2003) 387–394.